International Journal of Dental Research and Allied Sciences
2021, Volume 1, Issue 2, Page No: 26-38

Available online at: www.tsdp.net

ISSN: 3062-3502

Original Article

Effect of Argon Plasma Bioactivation on Titanium Implants in Graft-Free Maxillary Sinus Lifting: A Histological Study in Rabbits

Daan de Vries[1], Emma van Dijk[1]*

[1]Department of Oral and Maxillofacial Surgery, Rijnstate Hospital, Arnhem, Netherlands.

***E-mail** ✉ emmavandijk.real@yahoo.com

Received: 18 June 2021; **Revised:** 27 September 2021; **Accepted:** 28 September 2021

ABSTRACT

Surface modification of titanium implants using argon plasma has been shown to enhance their hydrophilicity and cellular adhesion, promoting increased bone deposition on both implant and graft surfaces. Experimental models have demonstrated that, following sinus augmentation, spontaneous sinus mucosa perforations may occur over time near implants and graft particles. The purpose of this study was to assess whether argon plasma treatment of implant surfaces influences bone apposition and the incidence of sinus mucosa perforations. Bilateral sinus lift surgeries were performed in sixteen rabbits. Implants either treated with argon plasma or left untreated (controls) were inserted simultaneously, without graft materials. After 8 weeks, histological examinations were conducted. Collapse of the sinus mucosa occurred at all implant sites. Of thirty-two implants, twenty-four showed mucosal perforations at the apex, and several also presented perforations along the threads. Nearly all implants were surrounded by thinned mucosa (thickness < 40 µm). The apical 2.6–2.9 mm segments lacked osseointegration, with approximately 1.3 mm exposed to the sinus cavity. No statistically meaningful differences were detected between the treated and control implants. Both argon plasma-treated and untreated implants led to mucosal injury and perforation through direct contact. Argon plasma surface modification did not alter the final outcomes.

Keywords: Animal model, Sinus lift, Bone regeneration, Schneiderian membrane, Histological evaluation

How to Cite This Article: de Vries D, van Dijk E. Effect of Argon Plasma Bioactivation on Titanium Implants in Graft-Free Maxillary Sinus Lifting: A Histological Study in Rabbits. Int J Dent Res Allied Sci. 2021;1(2):26-38. https://doi.org/10.51847/kv0PohKOhg

Introduction

Elevation of the maxillary sinus floor is frequently performed to augment bone volume in the atrophic posterior maxilla, facilitating implant placement. Implant-supported restorations in such sites have demonstrated high success rates [1, 2]. Nevertheless, reliable treatment outcomes rely on accurate cone beam computed tomography (CBCT) analysis to evaluate anatomic features [3–6] and detect septa or sinus pathologies [7, 8]. Sinus mucosa thickness can vary depending on apical infections, failed endodontic therapy, advanced caries, or periodontal bone loss [9]. The presence of septa may further complicate the surgical process, emphasizing the need for precise three-dimensional evaluation [10]. It is well established that, without additional interventions, the subantral space created during mucosa elevation tends to diminish over time [11, 12]. To prevent this reduction, biomaterials [13], various devices [14–17], or implants [18–22] are commonly utilized.

Simultaneous sinus elevation and implant placement without grafting has been described as a predictable approach with high success rates [23]. However, one clinical study found that bone gain did not always extend to the implant apex, leaving part of the implant unsupported by bone [24]. Similar findings were observed in a monkey model [21], where implants with moderately rough surfaces placed immediately after graft-free sinus augmentation showed mucosal collapse onto the apex and threads after one month.

Osseointegration from the sinus floor to the apex did not progress between 20 and 30 days, suggesting that mucosal collapse restricted bone growth at the implant tip. Roughly 3 mm of the apical region remained unintegrated within the sinus cavity. Conversely, in a rabbit study using grafts [25], less than 1 mm of the implant apex remained unintegrated after 8 weeks.

Among sinus lift complications, mucosal perforation is the most frequent [26–29]. Some clinical protocols intentionally perforate the sinus membrane during implant placement to achieve bicortical stability and maximize crestal bone use [30, 31]. Nevertheless, when implants are placed with their apices protruding beyond the elevated sinus floor, the subsequent condition of the sinus mucosa becomes a concern. Prior experimental data revealed spontaneous mucosal perforations following sinus augmentation around both implants [32] and graft materials [32, 33], suggesting that implants placed without grafts could face a higher risk of mucosal perforation over time.

Improving the osteoconductivity of implant surfaces might eliminate the need for grafts by promoting faster bone growth toward the apex. Numerous studies have examined surface treatments using diverse techniques [34–38]. Animal models evaluating different surface textures in marginal defects [39–41] indicated that surface modification enhances osteoconductivity. Furthermore, ultraviolet (UV) treatment has been reported to improve implant osseointegration [42]. Argon plasma treatment of titanium surfaces induces physicochemical changes that enhance wettability, protein adsorption, and cellular attachment [43], as confirmed by increased cell adhesion [44–46]. These effects are attributed to alterations in the surface electric field that attract charged proteins and osteoblasts [47]. Enhanced fibroblast and osteoblast adhesion to abutments [48] and grafts [49] has also been observed. Animal studies further demonstrated greater bone deposition on argon plasma-treated implants [50] and graft materials [51–53] during early healing phases.

Given these potential benefits, argon plasma treatment might theoretically reduce mucosal damage and spontaneous perforations by accelerating bone formation, thereby limiting mucosa–implant contact. Accordingly, the present study investigated the impact of argon plasma treatment on bone formation and the prevalence of sinus mucosa injuries and perforations.

Materials and Methods

Ethical compliance

Approval for this experiment was granted on April 8, 2019, by the Research Ethics Committee, Faculty of Dentistry, Ribeirão Preto, University of São Paulo (Protocol No. 2019.1.111.58.9). The research procedures followed the ARRIVE standards, and all steps involving animals complied strictly with Brazilian animal welfare legislation.

Experimental animals

Sixteen male New Zealand white rabbits, aged between 5 and 6 months and weighing approximately 3.5–4.0 kg, were selected for the study.

Design of the experiment

A split-mouth randomized design was used to reduce inter-animal variability. Each rabbit underwent bilateral sinus elevation. On one side, an argon plasma–treated implant (test) was placed, while on the opposite side, an untreated implant (control) was installed. Both were inserted through the antrostomies without adding any grafting materials.

Sample size determination

The sample estimation was based on earlier data from a canine study where implants were positioned in the edentulous ridge [50]. In that trial, a significant increase in bone-to-implant contact was observed for the argon plasma–treated implants using six subjects. Considering the present design—focused on sinus mucosa perforations—and potential losses, the number was expanded to sixteen rabbits.

Randomization and masking procedures

Random sequence generation took place electronically on July 26, 2019 (http://www.randomization.com) by an investigator (SPX) who did not participate in animal management or surgeries. Group allocations were placed in sealed opaque envelopes and only revealed to the surgeon (VFB) once both sinus antrostomies were prepared and the mucosa elevated. The histological evaluator (DB) was blinded to treatment allocation throughout the analysis.

Implant specifications and argon plasma activation

Implant size selection was based on previous studies conducted by the same research group in rabbits [25, 54]. Thirty-two tapered titanium grade IV implants (Five; Leader Medica, Padua, Italy) were utilized, each 5 mm in length and 3.35 mm in coronal diameter, all with the same macrogeometry **(Figure 1)** and double acid–etched surface texture. Sixteen implants received argon plasma treatment. The implants were sterilely unsealed to expose their surface to plasma gas discharge. Activation was conducted using a vacuum cold plasma unit (Plasma R, Sweden & Martina, Padua, Italy). Argon gas (>99.9990% purity) was supplied at

10 Pa base pressure, reaching an operational pressure of 20 Pa, and each implant was treated for 12 minutes [39].

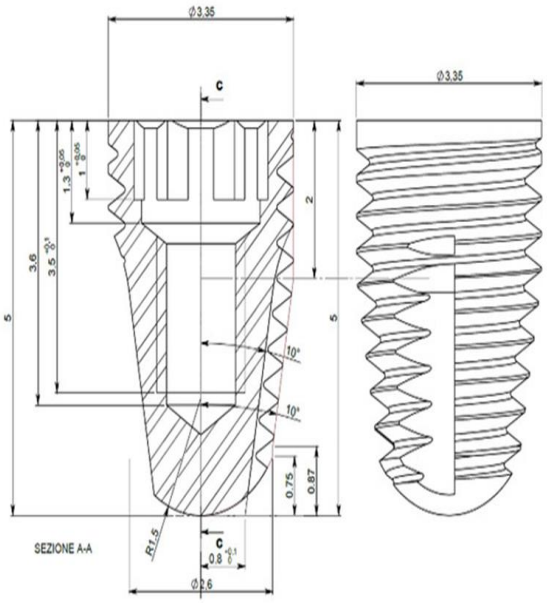

Figure 1. Technical implant dimensions.

Surgical technique

All interventions were performed by a single experienced surgeon (VFB). Sedation was initiated with subcutaneous acepromazine (1.0 mg/kg; Acepran®, Vetnil, Louveira, SP, Brazil). Intramuscular injections of xylazine (3.0 mg/kg; Dopaser®, Hertape Calier, Juatuba, MG, Brazil) and ketamine hydrochloride (50 mg/kg; Ketamin Agener, União Química Farmacêutica Nacional S/A, Embu-Guaçú, SP, Brazil) followed. Supplemental anesthesia (0.6 mL of Mepivacaine Hydrochloride 2% with 1:100,000 epinephrine; Mepiadre®, Nova DFL, Rio de Janeiro, Brazil) was administered locally.

After shaving and disinfecting the dorsal nasal region, a 2.5 cm midline incision was made. The soft tissues and periosteum were lifted to expose the nasal bone. Round openings (3.0 mm diameter) were created bilaterally using twist drills. Each antrostomy center was positioned about 5 mm lateral to the nasal–incisal suture and 10 mm anterior to the nasal–frontal suture, corresponding to the sinus cavity while avoiding the nasal passage. The sinus mucosa was gently detached from the lateral, medial, mesial, and distal walls using a fine elevator (718-EN1; Bontempi Strumenti Chirurgici, San Giovanni in Marignano, RN, Italy) to minimize tension. Alignment pins were used to check mucosal flexibility and integrity, inserted up to 5 mm below the cortical bone. Subsequently, the implants—test and control—were inserted randomly **(Figures 2b and 2c)**. Primary fixation was obtained manually by engaging the nasal bone without fracturing the delicate cortical layer.

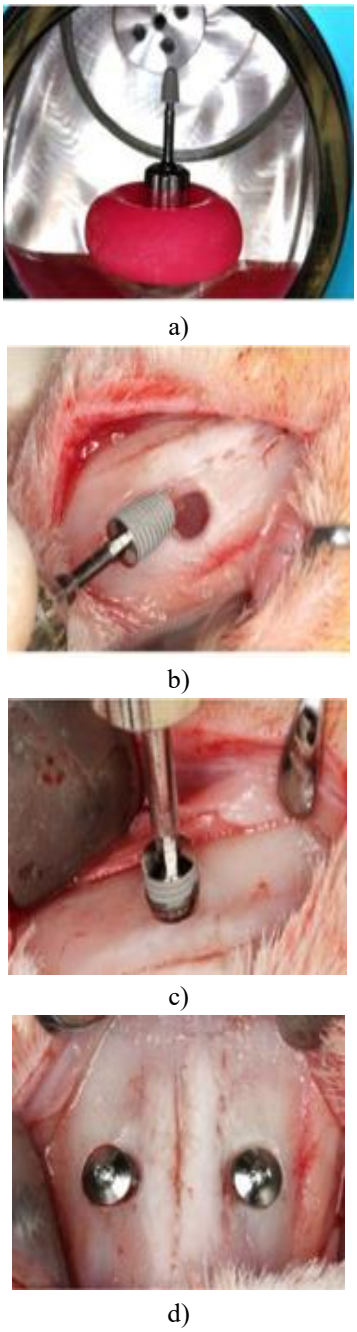

a)

b)

c)

d)

Figure 2. Sequence of implant installation: (a) Argon plasma device; (b) prepared osteotomy; (c) implant insertion; (d) placement of cover screws.

After implant installation, cover screws were applied **(Figure 2d)**. The periosteum was sutured using resorbable thread (Polyglactin 910 5-0, Vicryl®, Ethicon, Johnson & Johnson, São José dos Campos, Brazil), and the skin was closed with nylon sutures (Ethilon 4-0®, Ethicon, Johnson & Johnson, São José dos Campos, Brazil).

Maintenance procedures

Each animal was housed separately in climate-controlled conditions with unrestricted access to food and water. Throughout the experimental period, veterinarians continually monitored the animals' general condition, including wound healing and physiological parameters. For three consecutive days after surgery, all animals were treated with postoperative medications: ketoprofen 1% (Ketofen, Bimeda-Mogivet Farmacêutica SA, 3.0 mg/kg, intramuscularly; Monte-Mor, São Paulo, Brazil) and tramadol hydrochloride (1 mg/kg, subcutaneously; Halexlstar, Goiânia, Goiás, Brazil).

Animal euthanasia

Following an 8-week period, anesthesia was induced using xylazine (3.0 mg/kg, IM, Anasedan®, Sespo Indústria e Comércio LTDA, Paulínia, São Paulo, Brazil) in combination with ketamine (50.0 mg/kg, IM, Dopaser®, Sespo Indústria e Comércio LTDA, Paulínia, São Paulo, Brazil). Once deeply anesthetized, euthanasia was performed by exposing the animals to carbon dioxide (CO_2) within a sealed transparent acrylic chamber.

Tissue processing for histology

The entire nasal complex, including both treated maxillary sinuses, was excised en bloc and immediately fixed in buffered 10% formaldehyde solution.

Specimens were subsequently passed through graded ethanol series for dehydration, embedded in LR White™ Hard Grade resin (London Resin Co Ltd., Berkshire, UK), and polymerized. Using precision cutting and grinding equipment (Exakt, Apparatebau, Norderstedt, Germany), two longitudinal sections were obtained from each sample and thinned to approximately 50–60 µm. The slides were stained with either toluidine blue or Stevenel's blue and alizarin red for microscopic assessment.

Histometric assessments

A single experienced observer (DB) conducted the microscopic evaluations on both slides using an Eclipse Ci microscope (Nikon Corporation, Tokyo, Japan) equipped with a video camera (Digital Sight DS-2Mv, Nikon Corporation, Tokyo, Japan) and analyzed via NIS-Elements D software (v5.11.00, Nikon Corporation, Tokyo, Japan).

The following reference points were identified **(Figure 3)**: B—most coronal and apical bone-to-implant contacts; Ab—most apical contact; Ae—apical edge of perforated mucosal epithelium; X—implant apex. Definitions were as follows: (i) pristine mucosa, width of intact sinus mucosa measured on lateral and medial walls outside the elevated region; (ii) apical perforation, mucosal discontinuity involving the implant apex; (iii) thread perforation, mucosal break including any thread; (iv) thinned mucosa, sinus mucosa at the elevated zone less than 40 µm thick.

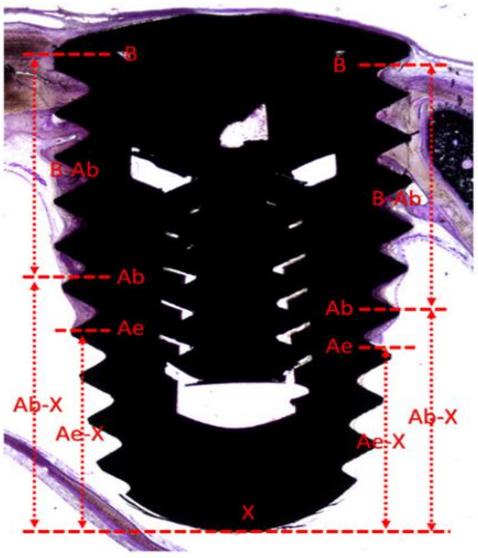

Figure 3. Reference map showing points B, Ab, Ae, and X, and vertical distances measured: B–Ab (osseointegration height), Ab–X (apical non-integrated implant region), and Ae–X (implant portion not covered by mucosa).

At ×100 magnification, the following parameters were measured: B–Ab, Ab–X, and Ae–X.

At ×400 magnification, the following were quantified: (i) perforations at apex and threads, (ii) width and count of thinned mucosa areas, and (iii) thickness of pristine mucosa.

Statistical processing

Primary measurement variables were Ab–X and Ae–X; secondary ones included the count of perforations and thinned mucosal regions. All data were analyzed with Prism 9.1.1 (GraphPad Software, LLC, San Diego, CA, USA). Group differences were tested using the Wilcoxon method ($p < 0.05$), and correlations between Ab–X and Ae–X were assessed via Spearman's two-tailed test ($p < 0.05$; 95% CI).

Tables report mean ± SD, median, and 25th/75th percentiles; in-text results mention only mean values.

Results and Discussion

Qualitative histological findings

Implant orientation relative to the sinus and nasal cavities is presented in **Figure 4**.

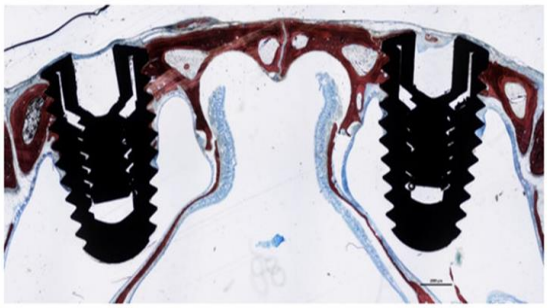

Figure 4. Photomicrograph showing implant placement within the sinus cavity; primary stability derived from nasal cortical bone.

After 8 weeks, histological observation revealed the sinus mucosa had collapsed around the implant body **(Figure 5a)**.

a)

b)

Figure 5. Ground section micrographs: (a) sinus mucosa collapsed around implant body with limited bone growth from nasal cortex toward apex; (b) bone-to-implant contact evident on medial sinus wall. Stains: (a) toluidine blue; (b) Stevenel's blue and alizarin red.

Out of 32 total implants, only 8 lacked apical perforations. Of these, 2 had exposed threads, leaving merely 6 implants fully encased by mucosa. In several samples, epithelial continuity was disrupted at both apical and thread levels. The perforated sites were lined with tapered epithelial cells and demonstrated variable inflammatory infiltrate intensities in both groups **(Figures 6a–6c)**.

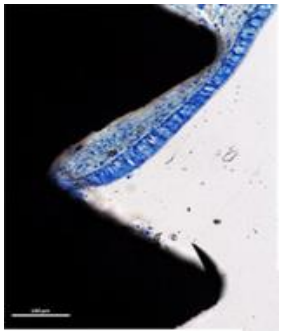

a)

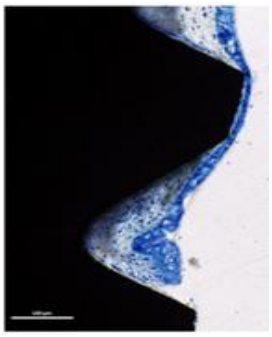

b)

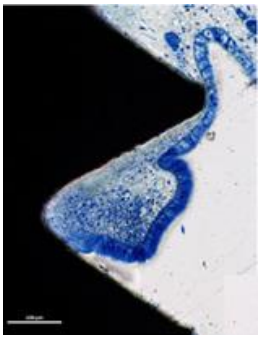

c)

Figure 6. Microscopic views of ground sections.

Around the perforated regions, elongated epithelial borders were visible, showing either mild (A,B) or intense (C) inflammatory cell presence in both examined groups. Staining: Stevenel's blue and Alizarin red.

When the implants lacked apical perforations, the apical area was occasionally positioned against the inner bone surface, promoting bone anchorage on the medial side of the fixture **(Figure 5b)**. This close contact likely aided in preserving the continuity of the sinus lining.

Of the thirty-two evaluated implants, twenty-seven demonstrated regions where the mucosa was markedly thinned, measuring below 10 µm in thirty-two separate locations. Only five implants that were deeply exposed within the sinus cavity showed no thinning. These thin mucosal areas were typically linked to the crest of the implant threads and showed varying microscopic appearances depending on the extent of tissue alteration. In the mildly affected sites, the thread tips

displaced or compressed vessels and mucous glands but left the pseudostratified ciliated columnar epithelium intact **(Figure 7a)**. With greater reduction in thickness, the connective tissue layer, glands, and vessels became entirely distorted **(Figure 7b)**, and with further progression, the epithelium itself became thinner with evident loss of cilia and goblet cells **(Figures 7c and 8a)**.

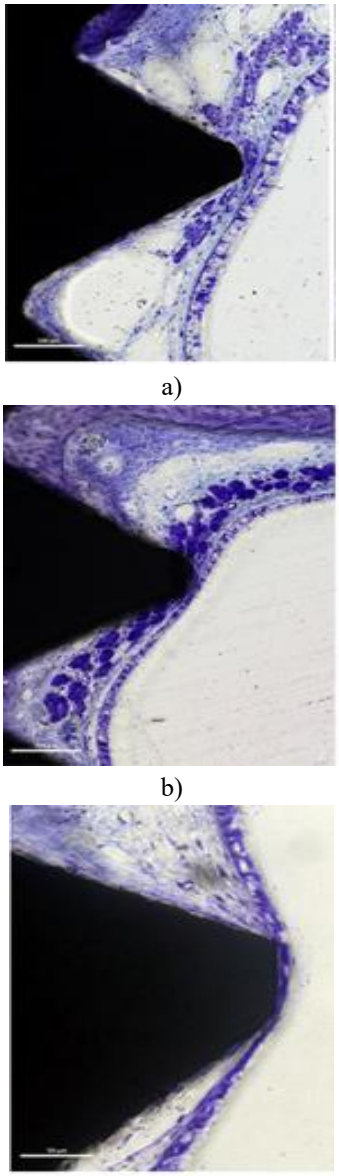

Figure 7. Microscopic images of ground sections.
(a) Early stage: thread tips displaced glands and vessels but epithelium remained unaffected.
(b) Intermediate stage: complete distortion of the submucosal tissue and vascular structures.
(c) Advanced stage: epithelial layer thinning with disappearance of goblet cells and cilia.
(a–c) Toluidine blue stain.

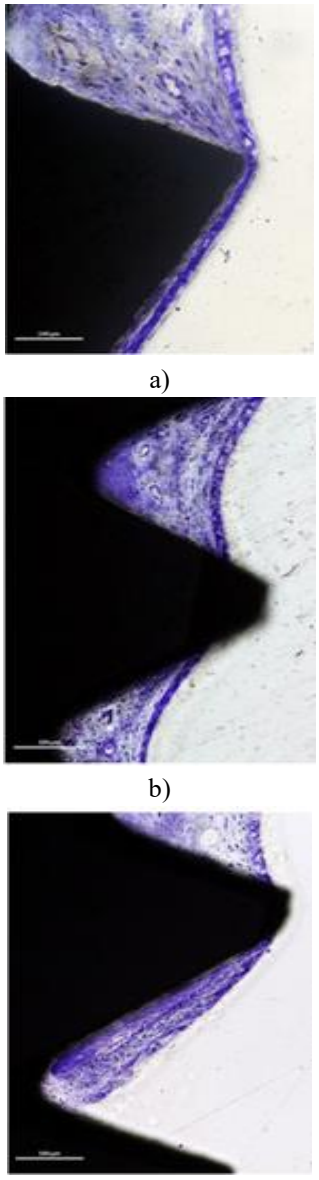

Figure 8. Microscopic images of ground sections.
(a) Thinned mucosa located near the terminal threads and apex (bottom).
(b, c) Mucosa adjacent to exposed threads usually showed less inflammatory reaction than areas with apical exposure.
(a–c) Toluidine blue stain.

The sinus lining in contact with exposed threads generally contained fewer inflammatory cells than at apical exposure sites **(Figures 8b and 8c)**.

Epithelial cells were often detected adjacent to the uncovered submucosa **(Figures 9a–9c)**. Partial repair activity was noted, frequently accompanied by overproduction of mucus by goblet cells **(Figure 9a)**. Additionally, in some regions, the epithelium appeared folded in a coronal direction under the neighboring mucosal tissue **(Figure 9c)**.

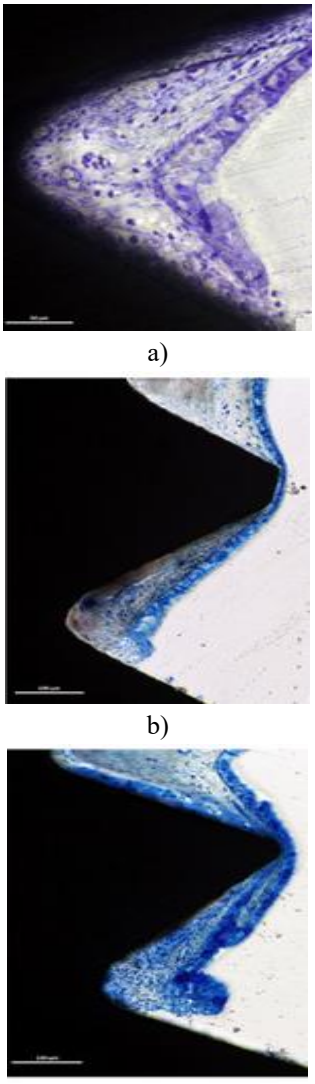

a)

b)

c)

Figure 9. Microscopic views of ground sections.
(a, b) Reparative epithelial proliferation attempting to cover the exposed submucosa, often with goblet cell overactivity (a).
(c) The epithelial sheet folding coronally beneath the nearby mucosal surface.
(a) Toluidine blue staining; (b, c) Stevenel's blue and Alizarin red.

Inflammatory foci within the sinus cavity (indicative of sinusitis) were uncommon and appeared together with different grades of mucosal degeneration **(Figures 10a and 10b)**.

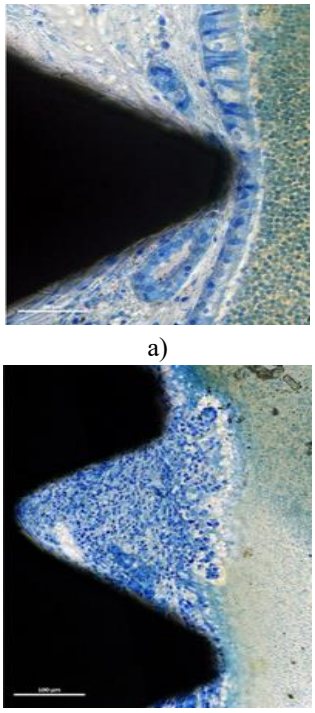

a)

b)

Figure 10. Microscopic views of ground sections.
(a, b) Rare intra-sinus inflammatory areas associated with degenerative alterations of the sinus mucosa.
Stain: Stevenel's blue and Alizarin red.

Quantitative histologic assessment

The mean vertical distance B–Ab (indicating osseointegration height) averaged 1.97 mm in the plasma-treated samples and 1.81 mm in the untreated controls **(Table 1)**. Distances Ab–X and Ae–X were 2.65 mm and 1.32 mm in the plasma group, versus 2.90 mm and 1.31 mm in controls. None of these variances reached statistical significance.

Table 1. Histometric values (mm) for bone and mucosal interfaces on implant surfaces.

Group	Statistic	B-Ab	Ab-X	Ae-X
Plasma	Mean ± SD Median (25%; 75%)	1.97 ± 0.91 1.84 (1.22; 2.61)	2.65 ± 0.94 2.72 (1.98; 3.39)	1.32 ± 1.31 0.84 (0.08; 2.39)
Control	Mean ± SD Median (25%; 75%)	1.81 ± 0.82 1.67 (1.17; 2.23)	2.90 ± 0.92 3.12 (2.38; 3.64)	1.31 ± 1.36 0.86 (0.09; 2.32)
Wilcoxon Test	p-value	0.678	0.520	0.891

B: uppermost bone–implant contact; Ab: most apical bone contact; X: implant apex; Ae: apical mucosal contact. $p < 0.05$.

Perforation frequencies at the apices and along the threads were nearly identical between groups—12 apices and 15 threads for the plasma condition, compared with 12 apices and 18 threads for controls **(Table 2)**. Thinning sites totaled 55 and 58, respectively. No statistically meaningful differences emerged. Correlation between Ab–X and Ae–X reached $r = 0.69$ ($p = 0.004$; CI 0.28–0.89) for plasma

and r = 0.67 (p = 0.005; CI 0.25–0.88) for the control specimens.

Table 2. Frequency of apical and thread perforations with mucosal thinning counts.

Group	Apical Perforations	Thread Perforations	Sites of Thinning
Plasma	12	15	55
Control	12	18	58
Wilcoxon Test	1.000	1.000	0.826

$p < 0.05$.

Average mucosal thinning measured 14 µm in the plasma group and 15 µm in controls **(Table 3)**. The narrowest sections reached 10 µm and 8 µm, respectively. Mean intact mucosa thicknesses were 82 µm for plasma-treated and 79 µm for control samples. None of these differences were significant.

Table 3. Measurements (µm) for mean, minimal, and intact mucosa thickness.

Group	Statistic	Thinned Mucosa Width	Thinnest Mucosa Width	Intact Mucosa
Plasma	Mean ± SD Median (25%; 75%)	14 ± 9 15 (9; 21)	10 ± 9 7 (2; 19)	82 ± 15 83 (68; 93)
Control	Mean ± SD Median (25%; 75%)	15 ± 8 16 (9; 21)	8 ± 7 7 (3; 11)	79 ± 15 77 (74; 87)
Wilcoxon Test	p-value	0.592	0.608	0.440

$p < 0.05$.

This study investigated whether applying argon plasma to implant surfaces could affect new bone formation or influence the occurrence of sinus membrane perforations. The analysis revealed that plasma exposure had no detectable influence on any of the recorded measurements.

Previous in vitro evidence indicates that the chance of contamination, even under clinical conditions, is essentially nonexistent [55]. In an animal trial using edentulous dog mandibles, no postoperative infections were reported [50]. That research compared two argon plasma–treated implants with two untreated controls. After two months of healing, a significant increase in bone-to-implant contact (BIC%) was observed in treated implants (72.5%) compared with untreated ones (64.7%). When the same surface activation method was applied to xenograft granules used for sinus floor elevation in rabbits [51], only the areas furthest from the native sinus walls exhibited any improvement. Another rabbit model using β-TCP/HA granules also showed a modest rise in bone formation following plasma treatment [52], though the intergroup difference remained statistically insignificant. Likewise, no noticeable improvement in bone regeneration occurred when argon plasma was used on xenogeneic bone blocks fixed to the mandible of rabbits [53].

In this experiment, the sinus membrane sagged onto the implant bodies, causing several tears and a gradual downward shift from the apical toward the coronal portion of the implant. This mechanical displacement probably restricted the beneficial impact of plasma treatment on bone deposition that had been seen in prior studies [50]. In both experimental groups, approximately 1.3 mm of the apical segment was not covered by the mucosa, reducing the possibility for new bone growth. As a result, the most apical 2.7–2.9 mm of the implant remained unlined by bone tissue after 8 weeks. The positive correlation found between Ab–X and Ae–X supports this view. These findings align with earlier experimental [21] and clinical data [24], which recorded roughly 3 mm of implant protrusion beyond the reconstructed sinus floor. Conversely, a separate rabbit investigation where implants were inserted together with sinus elevation using DBBM particles found that less than 1 mm of the apical portion remained unintegrated after 8 weeks [25].

In both groups, multiple perforations occurred at the implant apex and along the threads. This agrees with a rabbit experiment in which implants were placed immediately after bilateral sinus grafting with either deproteinized bovine bone mineral (DBBM) or autogenous bone (AB) harvested from the tibia [32]. Tissue samples were analyzed after 7 and 40 days (six animals per time point). After 7 days, the sinus mucosa remained intact, with minimal contact at the implant surface. After 40 days, three perforations were found in two sinuses at AB sites and one perforation at a DBBM site. The higher frequency in AB sites was linked to its faster resorption, which encouraged the membrane to collapse over the implant. Yet, DBBM granules also caused mucosal tearing. In the same trial [32], after 7 days, six perforations were found in two sinuses filled with DBBM, while none were observed in AB particles. By 40 days, three perforations occurred in

DBBM-treated sinuses, and none in AB, except those already identified around the implants.

Similar findings were obtained in another rabbit experiment [33], where bilateral sinus lifts were carried out using DBBM granules of two different sizes without implant placement. Healing was studied at 2, 4, and 8 weeks (six animals at each stage). After 2 weeks, only one sinus with large granules exhibited a tear, but the number of perforations increased with time; after 8 weeks, three of six sinuses in the large-granule group and four of six in the small-granule group showed mucosal defects.

In the current study, the average mucosal thickness of undamaged sites was roughly 80 µm, which is comparable to previously published measurements [32, 33, 56]. The thinned areas (<40 µm) observed in both plasma-treated and control samples displayed deformation of structural components, including glands and blood vessels, which were compressed against the implant surface irregularities. Past studies have shown that the incidence of thinned mucosa rises progressively at both implant [32] and DBBM sites [33]. This pattern suggests that the sinus lining undergoes gradual atrophy, which can eventually lead to rupture. Here, mucosal thinning and tearing mainly appeared around implant apices and threads, whereas in graft-based models, the main causes were the sharp projections of the granules [32, 33].

Following sinus augmentation, the cavity often re-pneumatizes, producing a reduction in subantral volume. This process has been verified through overviews [57], systematic reviews [58, 59], randomized clinical trials in humans [60–63], and numerous animal investigations [11, 12, 21, 54, 64, 65]. Perforations have likewise been documented in non-implant devices designed to sustain sinus elevation in primate experiments [14–16].

Clinically, the protrusion of dental implants above the sinus floor rarely causes significant sinus complications. A systematic review [66] found that postoperative nosebleeds and membrane thickening were the most frequent issues, with only one reported episode of sinusitis, which resolved after antibiotic treatment. Moreover, implant extension (≤4 mm versus >4 mm) did not influence survival or complication rates. The same review reported a 95.6% survival rate for implants exposed in the sinus cavity without bone grafts, over an average observation period of about four years.

Experimental investigations in dogs have also been conducted to evaluate potential maxillary sinus complications arising from implants extending into the sinus cavity [67–69]. After a 5–6-month healing period, every implant showed full integration, and no pathological alterations were identified in any sinus. The observations from the current research, however, only partially align with those findings. Although all implants achieved integration, the development of new bone at the apical portion was minimal. In addition, inflammatory cell aggregates of varying sizes were detected in the connective tissue surrounding the perforation zones. The epithelial layer did not always fully cover these sites, leaving some soft tissue regions directly exposed to the sinus lumen. In a few instances, the epithelial tissue appeared folded inward, seemingly attempting to close the lesions. Rarely, localized sinusitis was also identified.

A key limitation of this study lies in the anatomical difference between species: the rabbit sinus membrane is approximately 80 µm thick, whereas in humans, it measures around 0.45–1 mm [70]. Nonetheless, the mucosal thinning observed here—together with data from previous reports—suggests that a comparable progressive thinning process could also occur in humans, eventually resulting in membrane perforation. A control group evaluated at baseline (time 0) would have been beneficial to assess whether surgical manipulation itself contributed to mucosal injury. Despite this, an alignment pin was used before implant insertion to test the membrane's elasticity, minimizing trauma. Incorporating tomographic or microtomographic imaging would further enhance the analysis by providing three-dimensional detail. Moreover, employing shorter and longer healing intervals could help clarify the tissue response sequence and identify possible soft tissue regeneration during repair attempts.

From a clinical perspective, the present findings imply that sinus membrane perforation may arise when implants extend beyond the newly formed sinus floor. However, despite this possibility, the success rate of such implants remains high, and complication frequency is low [66].

Conclusion

In summary, the sinus lining was compromised and perforated following direct contact with both treated and untreated implant surfaces. The argon plasma modification of the implant surface did not influence these biological outcomes.

Acknowledgments: None

Conflict of Interest: None

Financial Support: None

Ethics Statement: None

References

1. Pjetursson BE, Tan WC, Zwahlen M, Lang NP. A systematic review of the success of sinus floor elevation and survival of implants inserted in combination with sinus floor elevation. J Clin Periodontol. 2008;35(Suppl 8):216–40.
2. Del Fabbro M, Wallace SS, Testori T. Long-term implant survival in the grafted maxillary sinus: a systematic review. Int J Periodontics Restor Dent. 2013;33(6):773–83.
3. Lozano-Carrascal N, Salomó-Coll O, Gehrke SA, Calvo-Guirado JL, Hernández-Alfaro F, Gargallo-Albiol J. Radiological evaluation of maxillary sinus anatomy: a cross-sectional study of 300 patients. Ann Anat. 2017;214(1):1–8.
4. Kawakami S, Botticelli D, Nakajima Y, Sakuma S, Baba S. Anatomical analyses for maxillary sinus floor augmentation with a lateral approach: a cone beam computed tomography study. Ann Anat. 2019;226(1):29–34.
5. Sakuma S, Ferri M, Imai H, Fortich Mesa N, Blanco Victorio DJ, Apaza Alccayhuaman KA, et al. Involvement of the maxillary sinus ostium (MSO) in the edematous processes after sinus floor augmentation: a cone-beam computed tomographic study. Int J Implant Dent. 2020;6(1):35.
6. Omori Y, Nakajima Y, Imai H, Yonezawa D, Ferri M, Apaza Alccayhuaman KA, et al. Influence of anatomical parameters on the dimensions of the subantral space and sinus mucosa thickening after sinus floor elevation: a retrospective cone beam computed tomography study. Dent J. 2021;9(7):76.
7. Maestre-Ferrín L, Galán-Gil S, Rubio-Serrano M, Peñarrocha-Diago M, Peñarrocha-Oltra D. Maxillary sinus septa: a systematic review. Med Oral Patol Oral Cir Bucal. 2010;15(2):e383–6.
8. Kato S, Omori Y, Kanayama M, Hirota A, Ferri M, Apaza Alccayhuaman KA, et al. Sinus mucosa thickness changes and ostium involvement after maxillary sinus floor elevation in sinus with septa: a cone beam computed tomography study. Dent J. 2021;9(8):82.
9. Kuligowski P, Jaroń A, Preuss O, Gabrysz-Trybek E, Bladowska J, Trybek G. Association between odontogenic and maxillary sinus conditions: a retrospective cone-beam computed tomographic study. J Clin Med. 2021;10(13):2849.
10. Malec M, Smektala T, Tutak M, Trybek G, Sporniak-Tutak K. Maxillary sinus septa prevalence and morphology: computed tomography-based analysis. Int J Morphol. 2015;33(1):144–8.
11. Asai S, Shimizu Y, Ooya K. Maxillary sinus augmentation model in rabbits: effect of occluded nasal ostium on new bone formation. Clin Oral Implants Res. 2002;13(4):405–9.
12. Xu H, Shimizu Y, Asai S, Ooya K. Grafting of deproteinized bone particles inhibits bone resorption after maxillary sinus floor elevation. Clin Oral Implants Res. 2004;15(1):126–33.
13. Corbella S, Taschieri S, Weinstein R, Del Fabbro M. Histomorphometric outcomes after lateral sinus floor elevation procedure: a systematic review of the literature and meta-analysis. Clin Oral Implants Res. 2016;27(9):1106–22.
14. Cricchio G, Palma VC, Faria PE, de Oliveira JA, Lundgren S, Sennerby L, et al. Histological findings following the use of a space-making device for bone reformation and implant integration in the maxillary sinus of primates. Clin Implant Dent Relat Res. 2009;11(Suppl 1):e14–e22.
15. Cricchio G, Palma VC, Faria PE, de Oliveira JA, Lundgren S, Sennerby L, et al. Histological outcomes on the development of new space-making devices for maxillary sinus floor augmentation. Clin Implant Dent Relat Res. 2011;13(3):224–30.
16. Schweikert M, Botticelli D, de Oliveira JA, Scala A, Salata LA, Lang NP. Use of a titanium device in lateral sinus floor elevation: an experimental study in monkeys. Clin Oral Implants Res. 2012;23(1):100–5.
17. Johansson LÅ, Isaksson S, Adolfsson E, Lindh C, Sennerby L. Bone regeneration using a hollow hydroxyapatite space-maintaining device for maxillary sinus floor augmentation—A clinical pilot study. Clin Implant Dent Relat Res. 2012;14(4):575–84.
18. Ellegaard B, Kølsen-Petersen J, Baelum V. Implant therapy involving maxillary sinus lift in periodontally compromised patients. Clin Oral Implants Res. 1997;8(4):305–15.
19. Lundgren S, Andersson S, Gualini F, Sennerby L. Bone reformation with sinus membrane elevation: a new surgical technique for maxillary sinus floor augmentation. Clin Implant Dent Relat Res. 2004;6(3):165–73.
20. Ellegaard B, Baelum V, Kølsen-Petersen J. Non-grafted sinus implants in periodontally compromised patients: a time-to-event analysis. Clin Oral Implants Res. 2006;17(2):156–64.

21. Scala A, Botticelli D, Faeda RS, Garcia Rangel IJ, Américo de Oliveira J, Lang NP. Lack of influence of the Schneiderian membrane in forming new bone apical to implants simultaneously installed with sinus floor elevation: an experimental study in monkeys. Clin Oral Implants Res. 2012;23(2):175–81.
22. Scala A, Botticelli D, Rangel IG Jr, de Oliveira JA, Okamoto R, Lang NP. Early healing after elevation of the maxillary sinus floor applying a lateral access: a histological study in monkeys. Clin Oral Implants Res. 2010;21(12):1320–6.
23. Silva LD, de Lima VN, Faverani LP, de Mendonça MR, Okamoto R, Pellizzer EP. Maxillary sinus lift surgery—with or without graft material? A systematic review. Int J Oral Maxillofac Surg. 2016;45(12):1570–6.
24. Cricchio G, Sennerby L, Lundgren S. Sinus bone formation and implant survival after sinus membrane elevation and implant placement: a 1- to 6-year follow-up study. Clin Oral Implants Res. 2011;22(11):1200–12.
25. Masuda K, Silva ER, Apaza Alccayhuaman KA, Botticelli D, Xavier SP. Histologic and micro-CT analyses at implants placed immediately after maxillary sinus elevation using large or small xenograft granules: an experimental study in rabbits. Int J Oral Maxillofac Implants. 2020;35(4):739–48.
26. Schwarz L, Schiebel V, Hof M, Ulm C, Watzek G, Pommer B. Risk factors of membrane perforation and postoperative complications in sinus floor elevation surgery: review of 407 augmentation procedures. J Oral Maxillofac Surg. 2015;73(7):1275–82.
27. Danesh-Sani SA, Loomer PM, Wallace SS. A comprehensive clinical review of maxillary sinus floor elevation: anatomy, techniques, biomaterials and complications. Br J Oral Maxillofac Surg. 2016;54(7):724–30.
28. Testori T, Weinstein T, Taschieri S, Wallace SS. Risk factors in lateral window sinus elevation surgery. Periodontol 2000. 2019;81(1):91–123.
29. Testori T, Yu SH, Tavelli L, Wang HL. Perforation risk assessment in maxillary sinus augmentation with lateral wall technique. Int J Periodontics Restor Dent. 2020;40(3):373–80.
30. Brånemark PI, Adell R, Albrektsson T, Lekholm U, Lindstrom J, Rockler B. An experimental and clinical study of osseointegrated implants penetrating the nasal cavity and maxillary sinus. J Oral Maxillofac Surg. 1984;42(8):497–505.
31. Nooh N. Effect of Schneiderian membrane perforation on posterior maxillary implant survival. J Int Oral Health. 2013;5(3):28–34.
32. Kato S, Botticelli D, De Santis E, Kanayama M, Ferreira S, Rangel-Garcia I Jr. Sinus mucosa thinning and perforation after sinus augmentation: a histological study in rabbits. Oral Maxillofac Surg. 2021;25(4):1–7.
33. Miki M, Botticelli D, Silva ER, Xavier SP, Baba S. Incidence of sinus mucosa perforations during healing after sinus lifting using deproteinized bovine bone mineral as grafting material: a histological evaluation in a rabbit model. Int J Oral Maxillofac Implants. 2021;36(4):660–8.
34. Abrahamsson I, Berglundh T, Linder E, Lang NP, Lindhe J. Early bone formation adjacent to rough and turned endosseous implant surfaces: an experimental study in the dog. Clin Oral Implants Res. 2004;15(4):381–92.
35. Buser D, Broggini N, Wieland M, Schenk RK, Denzer AJ, Cochran DL, et al. Enhanced bone apposition to a chemically modified SLA titanium surface. J Dent Res. 2004;83(7):529-33.
36. Favero R, Lang NP, Salata LA, Martins Neto EC, Caroprese M, Botticelli D. Sequential healing events of osseointegration at UnicCa® and SLActive® implant surfaces: an experimental study in the dog. Clin Oral Implants Res. 2016;27(2):203–10.
37. Bengazi F, Lang NP, Canciani E, Viganò P, Velez JU, Botticelli D. Osseointegration of implants with dendrimers surface characteristics installed conventionally or with Piezosurgery®: a comparative study in the dog. Clin Oral Implants Res. 2014;25(1):10–5.
38. Caneva M, Lang NP, Calvo-Guirado JL, Spriano S, Iezzi G, Botticelli D. Bone healing at bicortically installed implants with different surface configurations: an experimental study in rabbits. Clin Oral Implants Res. 2015;26(3):293–9.
39. Akimoto K, Becker W, Donath K, Becker BE, Sanchez R. Formation of bone around titanium implants placed into zero wall defects: pilot project using reinforced e-PTFE membrane and autogenous bone grafts. Clin Implant Dent Relat Res. 1999;1(2):98–104.
40. Botticelli D, Berglundh T, Persson LG, Lindhe J. Bone regeneration at implants with turned or rough surfaces in self-contained defects: An experimental study in the dog. J Clin Periodontol. 2005;32(5):448–55.

41. Rossi F, Lang NP, De Santis E, Morelli F, Favero G, Botticelli D. Bone-healing pattern at the surface of titanium implants: An experimental study in the dog. Clin Oral Implants Res. 2014;25(2):124–31.
42. Pesce P, Menini M, Santori G, Giovanni E, Bagnasco F, Canullo L. Photo and plasma activation of dental implant titanium surfaces: a systematic review with meta-analysis of pre-clinical studies. J Clin Med. 2020;9(9):2817.
43. Canullo L, Cassinelli C, Götz W, Tarnow D. Plasma of argon accelerates murine fibroblast adhesion in early stages of titanium disk colonization. Int J Oral Maxillofac Implants. 2013;28(4):957–62.
44. Rupp F, Gittens RA, Scheideler L, Marmur A, Boyan BD, Schwartz Z, et al. A review on the wettability of dental implant surfaces I: theoretical and experimental aspects. Acta Biomater. 2014;10(7):2894–906.
45. Ismail FS, Rohanizadeh R, Atwa S, Mason RS, Ruys AJ, Martin PJ, et al. The influence of surface chemistry and topography on the contact guidance of MG63 osteoblast cells. J Mater Sci Mater Med. 2007;18(4):705–14.
46. Lai HC, Zhuang LF, Liu X, Wieland M, Zhang ZY, Zhang ZY. The influence of surface energy on early adherent events of osteoblast on titanium substrates. J Biomed Mater Res A. 2010;93(1):289–96.
47. Kabaso D, Gongadze E, Perutková S, Matschegewski C, Kralj-Iglic V, Beck U, et al. Mechanics and electrostatics of the interactions between osteoblasts and titanium surface. Comput Methods Biomech Biomed Engin. 2011;14(6):469–82.
48. Garcia B, Camacho F, Peñarrocha D, Tallarico M, Perez S, Canullo L. Influence of plasma cleaning procedure on the interaction between soft tissue and abutments: a randomized controlled histologic study. Clin Oral Implants Res. 2017;28(10):1269–77.
49. Canullo L, Genova T, Rakic M, Sculean A, Miron R, Muzzi M, et al. Effects of argon plasma treatment on the osteoconductivity of bone grafting materials. Clin Oral Investig. 2020;24(8):2611–23.
50. Canullo L, Tallarico M, Botticelli D, Alccayhuaman KAA, Martins Neto EC, Xavier SP. Hard and soft tissue changes around implants activated using plasma of argon: a histomorphometric study in dog. Clin Oral Implants Res. 2018;29(4):389–95.
51. Hirota A, Yamada Y, Canullo L, Xavier SP, Baba S. Bioactivation of bovine bone matrix using argon plasma: An experimental study for sinus augmentation in rabbits. Int J Oral Maxillofac Implants. 2020;35(4):731–8.
52. Tanaka K, Botticelli D, Canullo L, Baba S, Xavier SP. New bone ingrowth into β-TCP/HA graft activated with argon plasma: a histomorphometric study on sinus lifting in rabbits. Int J Implant Dent. 2020;6(1):36.
53. Kanayama M, Botticelli D, Apaza Alccayhuaman KA, Yonezawa D, Silva ER, Xavier SP. The impact on the healing of bioactivation with argon plasma of a xenogeneic graft with adequate fixation but poor adaptation to the recipient site: an experimental study in rabbits. Int J Oral Maxillofac Implants. 2021;36(4):703–14.
54. De Santis E, Lang NP, Ferreira S, Rangel Garcia IJ Jr, Caneva M, Botticelli D. Healing at implants installed concurrently to maxillary sinus floor elevation with Bio-Oss® or autologous bone grafts: a histomorphometric study in rabbits. Clin Oral Implants Res. 2017;28(5):503–11.
55. Canullo L, Genova T, Pesce P, Nakajima Y, Yonezawa D, Mussano F. Surface bio-functionalization using plasma of argon could alter microbiological and topographic surface analysis of dental implants? Ann Anat. 2020;230(1):151489.
56. Iida T, Carneiro Martins Neto E, Botticelli D, Apaza Alccayhuaman KA, Lang NP, Xavier SP. Influence of a collagen membrane positioned subjacent the sinus mucosa following the elevation of the maxillary sinus: a histomorphometric study in rabbits. Clin Oral Implants Res. 2017;28(12):1567–76.
57. Ting M, Rice JG, Braid SM, Lee CYS, Suzuki JB. Maxillary sinus augmentation for dental implant rehabilitation of the edentulous ridge: a comprehensive overview of systematic reviews. Implant Dent. 2017;26(3):438–64.
58. Shanbhag S, Shanbhag V, Stavropoulos A. Volume changes of maxillary sinus augmentations over time: a systematic review. Int J Oral Maxillofac Implants. 2014;29(4):881–92.
59. Coopman R, Fennis J, Ghaeminia H, Van de Vyvere G, Politis C, Hoppenreijs TJM. Volumetric osseous changes in the completely edentulous maxilla after sinus grafting and lateral bone augmentation: a systematic review. Int J Oral Maxillofac Surg. 2020;49(12):1470–80.
60. Kawakami S, Lang NP, Iida T, Ferri M, Apaza Alccayhuaman KA, Botticelli D. Influence of the

position of the antrostomy in sinus floor elevation assessed with cone-beam computed tomography: A randomized clinical trial. J Investig Clin Dent. 2018;9(4):e12362.

61. Kawakami S, Lang NP, Ferri M, Alccayhuaman KAA, Botticelli D. Influence of the height of the antrostomy in sinus floor elevation assessed by cone beam computed tomography: a randomized clinical trial. Int J Oral Maxillofac Implants. 2019;34(2):223–32.
62. Hirota A, Lang NP, Ferri M, Mesa NF, Alccayhuaman KAA, Botticelli D. Tomographic evaluation of the influence of the placement of a collagen membrane subjacent to the sinus mucosa during maxillary sinus floor augmentation: a randomized clinical trial. Int J Implant Dent. 2019;5(1):31.
63. Imai H, Lang NP, Ferri M, Hirota A, Apaza Alccayhuaman AA, Botticelli D. Tomographic assessment on the influence on dimensional variations of the use of a collagen membrane to protect the antrostomy after maxillary sinus floor augmentation: a randomized clinical trial. Int J Oral Maxillofac Implants. 2020;35(2):350–6.
64. Caneva M, Lang NP, Garcia Rangel IJ, Ferreira S, Caneva M, De Santis E, et al. Sinus mucosa elevation using Bio-Oss® or Gingistat® collagen sponge: an experimental study in rabbits. Clin Oral Implants Res. 2017;28(Suppl 1):e21–e30.
65. Iida T, Silva ER, Lang NP, Apaza Alccayhuaman KA, Botticelli D, Xavier SP. Histological and micro-computed tomography evaluations of newly formed bone after maxillary sinus augmentation using a xenograft with similar density and mineral content of bone: an experimental study in rabbits. Clin Exp Dent Res. 2018;4(6):284–90.
66. Ragucci GM, Elnayef B, Suárez-López Del Amo F, Wang HL, Hernández-Alfaro F, Gargallo-Albiol J. Influence of exposing dental implants into the sinus cavity on survival and complications rate: a systematic review. Int J Implant Dent. 2019;5(1):6.
67. Jung JH, Choi BH, Zhu SJ, Lee SH, Huh JY, You TM, et al. The effects of exposing dental implants to the maxillary sinus cavity on sinus complications. Oral Surg Oral Med Oral Pathol Oral Radiol Endod. 2006;102(5):602–5.
68. Zhong W, Chen B, Liang X, Ma G. Experimental study on penetration of dental implants into the maxillary sinus in different depths. J Appl Oral Sci. 2013;21(6):560–6.
69. Elhamruni LM, Marzook HA, Ahmed WM, Abdul-Rahman M. Experimental study on penetration of dental implants into the maxillary sinus at different depths. Oral Maxillofac Surg. 2016;20(3):281–7.
70. Aimetti M, Massei G, Morra M, Cardesi E, Romano F. Correlation between gingival phenotype and Schneiderian membrane thickness. Int J Oral Maxillofac Implants. 2008;23(6):1128–32.